Open

Oncogene (2013) 32, 4519–4528

www.nature.com/onc

ORIGINAL ARTICLE

CpG island shore methylation regulates caveolin-1 expression in breast cancer

X Rao[1,2,12], J Evans[3,13], H Chae[3,14], J Pilrose[2], S Kim[3,14], P Yan[4], R-L Huang[5], H-C Lai[5], H Lin[6], Y Liu[6], D Miller[2], J-K Rhee[7], Y-W Huang[8], F Gu[9], JW Gray[10], TH-M Huang[9] and KP Nephew[1,2,11]

Caveolin-1 (Cav1) is an integral membrane, scaffolding protein found in plasma membrane invaginations (caveolae). Cav1 regulates multiple cancer-associated processes. In breast cancer, a tumor suppressive role for Cav1 has been suggested; however, Cav1 is frequently overexpressed in aggressive breast cancer subtypes, suggesting an oncogenic function in advanced-stage disease. To further delineate Cav1 function in breast cancer progression, we evaluated its expression levels among a panel of cell lines representing a spectrum of breast cancer phenotypes. In basal-like (the most aggressive BC subtype) breast cancer cells, Cav1 was consistently upregulated, and positively correlated with increased cell proliferation, anchorage-independent growth, and migration and invasion. To identify mechanisms of Cav1 gene regulation, we compared DNA methylation levels within promoter 'CpG islands' (CGIs) with 'CGI shores', recently described regions that flank CGIs with less CG-density. Integration of genome-wide DNA methylation profiles ('methylomes') with Cav1 expression in 30 breast cancer cell lines showed that differential methylation of CGI shores, but not CGIs, significantly regulated Cav1 expression. In breast cancer cell lines having low Cav1 expression (despite promoter CGI hypomethylation), we found that treatment with a DNA methyltransferase inhibitor induced Cav1 expression via CGI shore demethylation. In addition, further methylome assessments revealed that breast cancer aggressiveness associated with Cav1 CGI shore methylation levels, with shore hypermethylation in minimally aggressive, luminal breast cancer cells and shore hypomethylation in highly aggressive, basal-like cells. Cav1 CGI shore methylation was also observed in human breast tumors, and overall survival rates of breast cancer patients lacking estrogen receptor α (ERα) negatively correlated with Cav1 expression. Based on this first study of Cav1 (a potential oncogene) CGI shore methylation, we suggest this phenomenon may represent a new prognostic marker for ERα-negative, basal-like breast cancer.

Oncogene (2013) **32,** 4519–4528; doi:10.1038/onc.2012.474; published online 5 November 2012

Keywords: Cav1; CpG island shore; DNA methylation; breast cancer

INTRODUCTION

Caveolin-1 (Cav1) is a ubiquitous scaffolding protein that coats plasma membrane invaginations termed caveolae in various cell types.[1] A variety of proteins have been identified to interact with Cav1,[2] suggesting that Cav1 functions as a 'molecular hub' to integrate the activity of multiple signaling molecules, including Src-family tyrosine kinases, growth factor receptors (epidermal growth factor receptor), G protein and G-protein-coupled receptors, and H-Ras.[3–6] Interactions with the Cav1-scaffolding domain anchor these proteins in a restrained conformation, negatively regulating their activities.[7] In addition, locus D7S522 of human chromosome 7q31.1, the location of the Cav1 gene, is frequently deleted in human cancers,[8] further implicating Cav1 as a tumor suppressor. However, Cav1 upregulation has been observed in a variety of human cancers,[9] and Cav1 expression is a predictive marker of poor prognosis in cancer patients.[10] Furthermore, Cav1 upregulation has been correlated with metastatic potential[11–13] and multidrug resistance.[14,15] Thus, depending on the cellular context, Cav1 may also function as an oncogene.[10]

In breast cancer, Cav1 downregulation (compared with normal tissue) was observed, demonstrating an inverse correlation between Cav1 expression and tumor size,[16,17] and loss of Cav1 expression was associated with tamoxifen resistance.[18] Conversely, Cav1 was overexpressed in a subset of aggressive breast carcinomas,[19] including subsets of basal-like and metaplastic tumors and inflammatory breast cancers.[20] In breast cancer cell culture models, Cav1 downregulation was characteristic of luminal breast

[1]Interdisciplinary Biochemistry Graduate Program, Department of Molecular and Cellular Biochemistry, Indiana University, Bloomington, IN, USA; [2]Medical Sciences Program, School of Medicine, Indiana University, Bloomington, IN, USA; [3]Bioinformatics Program, School of Informatics and Computing, Indiana University, Bloomington, IN, USA; [4]NASRIllumina Sequencing Core, Comprehensive Cancer Center, The Ohio State University, Columbus, OH, USA; [5]Department of Obstetrics and Gynecology, Institute of Biomedical Informatics, National Yang-Ming University, Taipei City, Taiwan; [6]Department of Medical and Molecular Genetics, Indiana University School of Medicine, Indianapolis, IN, USA; [7]Interdisciplinary Program in Bioinformatics, Seoul National University, Seoul, Korea; [8]Department of Obstetrics and Gynecology, Medical College of Wisconsin, Milwaukee, WI, USA; [9]Department of Molecular Medicine, Cancer Therapy and Research Center, University of Texas Health Science Center, San Antonio, TX, USA; [10]Department of Biomedical Engineering, Oregon Health and Science University, Portland, OR, USA and [11]IU Simon Cancer Center and Departments of Cellular and Integrative Physiology, Indiana University School of Medicine, Indianapolis, IN, USA. Correspondence: Professor KP Nephew, Cellular and Integrative Physiology, Indiana University School of Medicine, 302 Jordan Hall, 1001 East Third Street, Bloomington, IN 47405-4401, USA.
E-mail: knephew@indiana.edu
[12]Current address: Department of Radiology, School of Medicine, Stanford University, Stanford, CA 94305, USA.
[13]Current address: Mayo Clinic, Rochester, MN 55905, USA.
[14]Current address: School of Computer Science and Engineering, Seoul National University, Seoul 151-742, Korea.
Received 26 January 2012; revised 10 August 2012; accepted 29 August 2012; published online 5 November 2012

cancer cells; in contrast, basal-like cells displayed overexpression of Cav1.[21–23] Despite these numerous observations, the role of Cav1 in breast cancer, and the mechanism(s) that regulates its diverse patterns of expression, remain to be fully established. To identify Cav1 gene regulatory mechanisms, we examined epigenetic changes associated with Cav1 expression in breast cancer.

Epigenetic alterations, including DNA methylation, histone modifications and nucleosome remodeling, are now considered hallmarks of all stages of cancer development.[24] DNA methylation, in the context of CpG dinucleotides, has profound effects on gene expression by influencing the accessibility of transcription factors to DNA, altering genetic stability and modifying genomic structure.[25,26] Specifically, DNA methylation of promoter CpG islands (CGIs) results in transcriptional silencing, and its dysregulation has an important role in oncogenesis and tumor progression.[24] However, as only about 70% of human genes contain a promoter CGI[27] and only 6.8% of CpGs reside within CGIs,[28] many potentially informative CpG sites remain to be examined. Recent work has shown that DNA methylation can directly silence genes with non-CGI promoters and contribute to the establishment of tissue-specific methylation patterns.[29] Furthermore, tissue- and cancer-specific differentially methylated regions occur more frequently within CGI shores, regions of relatively low CpG density that flank traditional CGIs (upto 2 kb distant), than within CGIs themselves,[30,31] suggesting the involvement of CGI shore methylation in tissue differentiation, epigenetic reprogramming and cancer.

In this study, using a panel of cell lines representing a spectrum of breast cancer phenotypes, we demonstrated dramatic upregulation and an oncogenic role for Cav1 in estrogen receptor α (ERα)-negative, basal-like cells, in which Cav1 supported cell proliferation, anchorage-independent growth, migration and invasion. To identify gene regulatory mechanism for Cav1, we investigated DNA methylation levels within the Cav1 promoter CGI and CGI shores. Differential CGI shore methylation strongly associated with Cav1 expression, a finding further confirmed in a panel of 30 breast cancer cell lines using methyl-CpG binding domain protein sequencing.[32] The methylome analysis further indicated an association between more aggressive breast cancer subtypes and Cav1 CGI shore hypermethylation. In addition, variable Cav1 CGI shore methylation was also observed in human breast tumors and overall survival rates of breast cancer patients lacking ERα negatively correlated with Cav1 expression. Based on this first report of CGI shore methylation of a potential oncogene, we suggest that Cav1 CGI shore methylation may represent a new prognostic marker for ERα-negative, basal-like breast cancer.

RESULTS

Oncogenic role of Cav1 in ERα-negative, basal-like breast cancer cells

Cav1 expression levels were examined in a panel of breast cancer cell lines representing several disease subtypes (Figure 1a), including luminal antiestrogen-sensitive MCF7 and BT-474, basal-like antiestrogen-resistant MDA-MB-231 and two antiestrogen-resistant MCF7-sublines, MCF7-F and MCF7-T.[33] MCF7-F, derived from MCF7, is resistant to both fulvestrant (a selective estrogen receptor downregulator) and tamoxifen (a selective estrogen receptor modulator) and have an ERα-negative and basal-like phenotype. MCF7-T is resistant to tamoxifen, but not to fulvestrant, and maintains an ERα-positive and luminal phenotype. Consistent with a previous report,[21] Cav1 mRNA levels were higher ($P<0.01$) in MDA-MB-231 cells than in MCF7 and BT-474 (Figure 1a). MCF7-T cells displayed decreased (2.5-fold, $P<0.01$) Cav1 expression, relative to its MCF7 parental cells, agreeing with a previous report.[18] However, Cav1 expression in MCF7-F cells was increased 4-fold ($P<0.01$) as compared with its parental MCF7 cells. Analysis of whole transcriptome RNA-seq data of MCF7, MCF7-T and MCF7-F cells confirmed this pattern of Cav1 expression (Supplementary Figure S1). Cav1 protein expression patterns, assessed by immunofluorescence staining, were similar to the mRNA expression patterns of Cav1 in these cell lines (Figure 1b).

To examine whether the distinct expression patterns of Cav1 in MCF7-T and MCF7-F were due to drug treatment, we investigated the effect of these drugs on endogenous Cav1 expression. The parental MCF7 cells were treated with 4-hydroxytamoxifen or fulvestrant for 8 days and Cav1 mRNA level was examined at the indicated time points. 4-hydroxytamoxifen repressed Cav1 expression ($P<0.01$, after day 2); however, no effect of fulvestrant on Cav1 levels was observed (Figure 1c). These results suggest that tamoxifen treatment may initially induce loss of Cav1 expression during the development of tamoxifen resistance, however, elevated Cav1 levels in fulvestrant resistant MCF7-F cells may result from long-term genetic and epigenetic alterations during the drug treatment and cell subtype transition (from luminal to basal).

To examine whether Cav1 expression directly associates with fulvestrant resistance, we ectopically overexpressed Cav1 in fulvestrant-sensitive MCF7 and MCF7-T cells, followed by fulvestrant treatment for 7 days. As expected, fulvestrant inhibited the growth of control MCF7 and MCF7-T cells (vector, empty vector-transfected) (Figure 1d and Supplementary Figure S2). Although the growth rate of Cav1-overexpressing cells was slightly reduced, compared with control cells when treated with DMSO, these cells were similarly growth-inhibited by fulvestrant, indicating that Cav1 alone could not confer resistance to this selective estrogen receptor downregulator (Figure 1d and Supplementary Figure S2). Furthermore, we examined cell response to 4-hydroxytamoxifen and concluded that Cav1 overexpression did not change cell sensitivity to the selective estrogen receptor modulator either (Supplementary Figure S3).

As MCF7-F cells showed increased clonogenicity,[33] and migration/invasion activity (Supplementary Figure S4) as compared with MCF7 and MCF7-T, we next assessed whether Cav1 expression contributed to the more aggressive basal-like phenotype. Ectopic Cav1 overexpression did not enhance clonogenic activity of MCF7 cells (Supplementary Figure S5a) and in fact decreased clonogenicity of MCF7-T cells (Supplementary Figure S5b). Elevated Cav1 expression significantly inhibited migration and invasion activity of MCF7 cells (Supplementary Figure S6a), while slightly increased invasiveness of MCF7-T cells (Supplementary Figure S6b). Therefore, overexpression of Cav1 was not sufficient to drive the more aggressive phenotype. However small interfering-mediated knockdown of Cav1 in MCF7-F cells significantly decreased cell proliferation (Figure 1e) and clonogenic activity (Figure 1f), as well as cell migration and invasion (Figure 1g). Similar results were also observed in MDA-MB-231 cells (Supplementary Figure S7). These results suggest that Cav1 expression is associated with breast cancer subtype and that this scaffolding protein has an oncogenic role in ERα-negative, basal-like breast cancer cells.

Direct role for CGI shore methylation in Cav1 gene expression

Although Cav1 has been reported to be upregulated by the DNA methyltransferase inhibitor 5-aza-CdR in prostate, lung and ovarian cancers,[34–36] hypermethylation of the Cav1 promoter CGI in human cancer appears to be rare, at only 6% of cervical[37] and 3.8% of colorectal cancers,[38] and entirely absent in primary ovarian tumors.[39] To further investigate the role of DNA methylation in Cav1 expression, we treated breast cancer cell lines displaying low Cav1 expression (MCF7, MCF7-T and BT-474) with 5-aza-CdR for 6 days. Although Cav1 mRNA levels increased ($P<0.01$) in all three cell lines (Figure 2a), that increase was not due to altered methylation of the Cav1 promoter CGI, which is

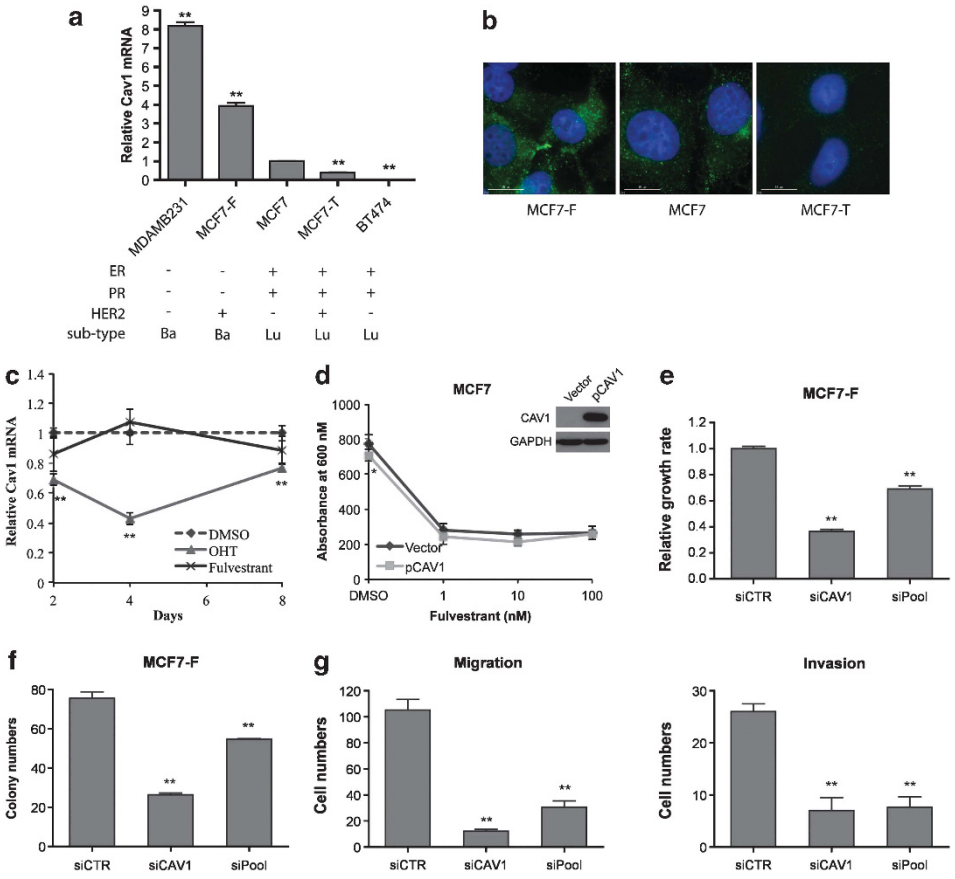

Figure 1. Cav1 is upregulated and has an oncogenic role in fulvestrant-resistant breast cancer cell lines. (**a**) Cav1 expression in a panel of antiestrogen-sensitive and -resistant breast cancer cell lines as measured by quantitative reverse transcription–PCR analysis and relative to its expression level in MCF7 cells (mean ± s.e., $n=3$). $^{**}P<0.01$. Molecular features of these lines are given: ER, estrogen receptor; PR, progesterone receptor; Ba, basal-like; Lu, luminal. (**b**) Immunofluorescence staining of Cav1 in MCF7, MCF7-T and MCF7-F cells. Cells were serum/E2 starved for 3 days, following by fluorescence microscopy (magnification ×60 oil immersion objective. Bar, 15 μm). (**c**) Effect of tamoxifen and fulvestrant on endogenous Cav1 expression. MCF7 were serum/E2 starved for 3 days and then treated with 1 μM 4-hydroxitamoxifen (OHT) or 100 nM fulvestrant for 8 days. Cav1 expression was detected at the indicated time point by reverse transcription–PCR, relative to it in dimethyl sulfoxide (DMSO)-treated cells (mean ± s.e., $n=3$). $^{**}P<0.01$. (**d**) Fulvestrant sensitivity of Cav1-overexpressing MCF7 cells. Cells were transfected with pCMV6-XL5 (vector) or Cav1 overexpression plasmid (pCAV1) and then treated with the indicated doses of fulvestrant for 7 days. Cell viability was determined by MTT assay (absorbance at 600 nm linearly correlated with cell number; mean ± s.e., $n=6$). The difference between vector-transfected cells and pCAV1-transfected cells was measured by Student's *t*-test. $^{*}P<0.05$. (**e**) Knockdown of Cav1 inhibits growth of MCF7-F cells. Cells were transfected with 50 nM control small interfering RNA (siCTR), or small interfering RNAs that target Cav1 (siCav1 and siPool) and cultured for 6 days. Cell viability was determined by MTT assay (mean ± s.e., $n=6$). $^{**}P<0.01$. (**f**) Knockdown of Cav1 inhibits clonogenicity of MCF7-F cells. Small interfering RNA-transfected cells were cultured in growth medium for 2 weeks and colonies containing >50 cells were scored (mean ± s.e., $n=3$). $^{**}P<0.01$. (**g**) Migration/invasion activity of MCF7-F cells (mean ± s.e., $n=3$). $^{**}P<0.01$.

constitutively hypomethylated, determined by both methylation-specific PCR and bisulfite sequencing (Figures 2b and c) Only sporadic methylation was observed in BT-474 cells, which had the lowest Cav1 expression. In contrast, methylation of the CpG sites located upstream of the Cav1 CGI (a '5′-CGI shore'),[30] was apparent (Figures 2b and d). Moreover, after 5-aza-CdR treatment, decreased Cav1 CGI shore methylation was observed (Figure 2d), indicating an association between shore methylation and expression.

To further investigate the relationship between Cav1 methylation and expression, we quantified Cav1 CGI and CGI shore DNA methylation levels by pyrosequencing, a fully quantitative methylation assessment, in the panel of antiestrogen-sensitive and -resistant cell lines displaying differential Cav1 expression levels (Figure 1a). Seven pairs of primers were designed to amplify different regions of Cav1, covering 10 and 18 CpG sites in the CGI shore and CGI, respectively (Supplementary Figure S8 and Supplementary Table S1). The analysis of individual CpG sites confirmed that the Cav1 CGI was hypomethylated in all cell lines (Supplementary Figure S9; summarized in Figure 3a). However, 5′-CGI shore methylation was decreased in the aggressive MDA-MB-231 and MCF7-F cells (median 2.7%, $P<0.05$ and median 9.6%, $P<0.01$, respectively), but not in less aggressive MCF7, MCF7-T and BT-474 (median 21.1%, 38.6% and 54.6%, respectively). Furthermore, 3′-CGI shore methylation inversely correlated with Cav1 expression in all these cell lines, with the lowest methylation level observed in MDA-MB-231 cells (median 2.9%, $P<0.01$ compared with all other cell lines), decreased ($P<0.01$) 3′-CGI shore methylation in MCF7-F cell (median 24.3%) and increased ($P<0.01$) 3′-CGI shore methylation in MCF7-T cells (median 64.2%) compared with MCF7 (median 42.1%). The highest ($P<0.01$) level of 3′-CGI shore methylation was observed in BT-474 cells (median 69.5% vs other cell lines except MCF7-T).

To determine whether shore methylation directly or indirectly influenced Cav1 gene expression, Cav1-low expressing cell lines (MCF7, MCF7-T and BT-474) treated with 5-aza-CdR were

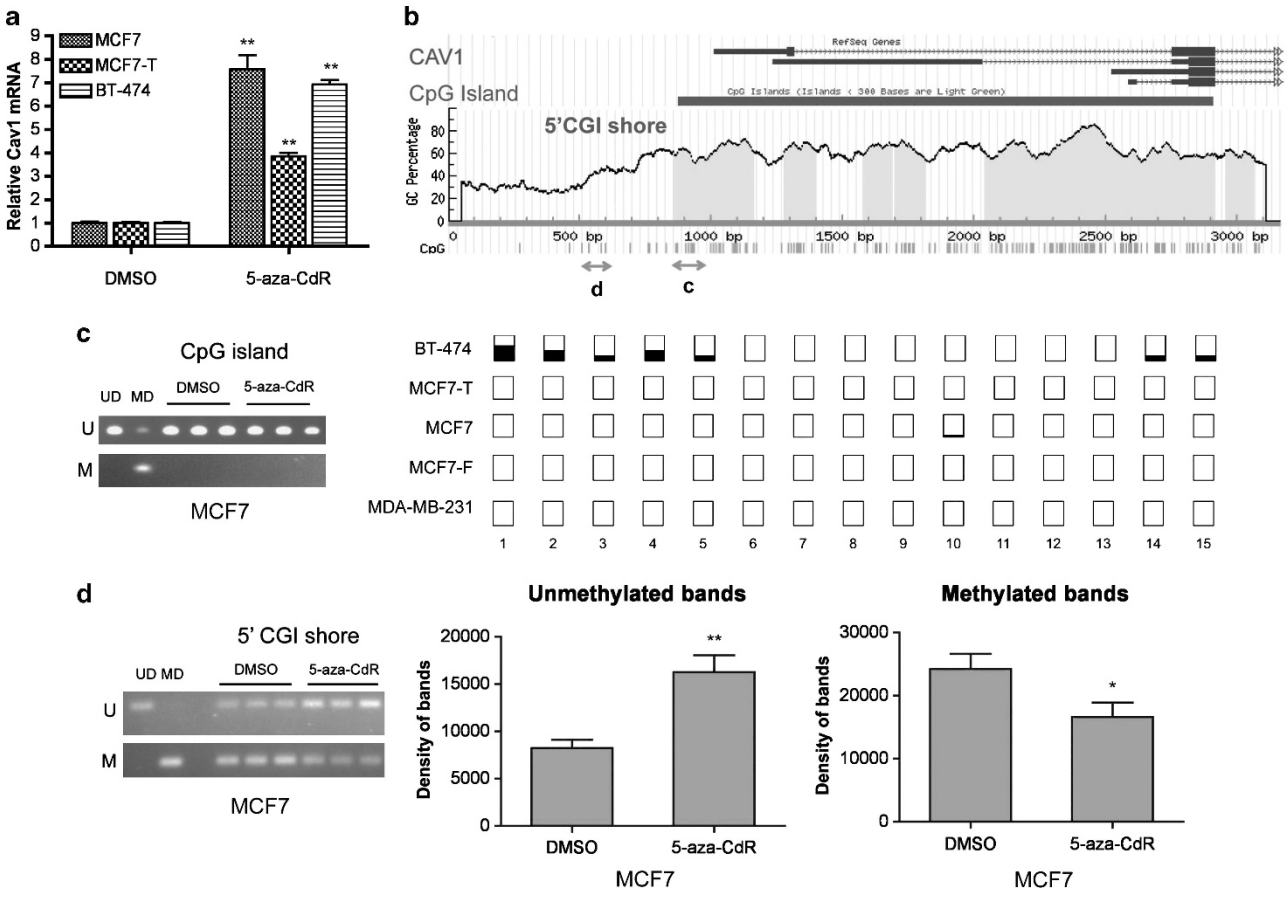

Figure 2. 5-aza-CdR restores Cav1 expression without affecting the hypomethylation of Cav1 CpG island (CGI). Cells were treated with 5 μM 5-aza-CdR for 6 days. Total RNA and genomic DNA were harvested for reverse transcription–PCR and bisulfite conversion. (**a**) Cav1 mRNA level measured by reverse transcription–PCR. The Cav1 level in DMSO treated cells was normalized to 1 (mean ± s.e., $n = 3$). $^{**}P < 0.01$. (**b**) UCSC genome browser view of Cav1 and distribution of CpG sites. The two two-headed arrows indicated the regions that are examined by methylation-specific PCR in (**c**) and (**d**). (**c**) CpG methylation on Cav1 CGI of MCF7 cell. Left: methylation-specific PCR result. UD, unmethylated DNA control. MD, methylated DNA control. U, results with primers specific for unmethylated sequence. *M*, results with primers specific for methylated sequence. Right: results of bisulfite genomic DNA sequencing covering the first 15 CpG sites on Cav1 CGI. Open squares indicate that CpG sites are fully unmethylated; partially filled squares indicate various degrees of CpG methylation. (**d**) CpG methylation on Cav1 5′-CGI shore. Left: methylation-specific PCR results of MCF7. Right: quantification of band density on the gel (mean ± s.e., $n = 3$). $^{*}P < 0.05$, $^{**}P < 0.01$.

subjected to pyrosequencing analysis. 5-aza-CdR decreased 5′- and 3′-CGI shore methylation levels in MCF7-T cells by an average of 56% (change from 39% to 17.1%) and 45% (change from 63 to 35%) ($P < 0.01$), respectively (Supplementary Figure S10; summarized in Figure 3b). Similar results were observed in MCF7 and BT-474 cells (Supplementary Figure S11). However, when MCF7-F cells, which have low Cav1 CGI shore methylation, were treated with 5-aza-CdR, Cav1 expression was only slightly increased (~1.8-fold, Supplementary Figure S12), compared with Cav1-low expressing cell lines (Figure 2a). Taken together, these results support a direct regulatory role of CGI shore methylation in Cav1 expression in breast cancer cells.

In addition, according to our bisulfite sequencing and pyrosequencing results, we did not observe any mutations in the Cav1 promoter CGI and CGI shores. Together with a recent study reporting lack of Cav1 gene mutations in human breast cancer,[40] the differential Cav1 expression and CGI shore methylation seems unlikely to be associated with DNA mutation.

Subtype-specific, Cav1 CpG island shore methylation patterns in breast cancer cell lines

To investigate whether CGI shore methylation is a common mechanism that regulates Cav1 expression, we performed genome-wide profiling of DNA methylation using methyl-CpG binding domain protein sequencing (see methods) on 30 breast cancer cell lines. The breast cancer cell lines were divided into two groups, 'Cav1-low' (12 luminal subtype and 3 basal A subtype) and 'Cav1-high' (15 basal subtype), based on our previous findings.[21] The DNA methylation landscapes of these cell lines indicated that Cav1 promoter CGI was hypomethylated in almost all cell lines, regardless of Cav1-expression level. However, hypermethylation of Cav1 CGI shores was observed mostly in Cav1-low lines (Figure 4).

A summary of DNA methylation around the Cav1 promoter CGI for luminal and basal subtype cells is shown in Figure 5a. DNA methylation in luminal/Cav1-low cells demonstrated two major peaks at the CGI shore regions and a sub-peak at the CGI; in contrast, the two major DNA methylation peaks at the CGI shore were dramatically lower in basal/Cav1-high lines. By integrating the methylome data with Cav1 mRNA expression profiles, we found that CGI shore methylation within 500 bp of CGI showed a strong negative correlation with Cav1 expression ($r < -0.7$), while a weak negative correlation ($r > -0.6$) was seen for CGI methylation or CGI shore methylation within 2 kb of the CGI (Figure 5b). These findings indicate that Cav1 CGI shore hypermethylation is a common event in luminal breast cancer and strongly associates with Cav1 gene repression. As Cav1 expression strongly associates with the basal-like subtype, we

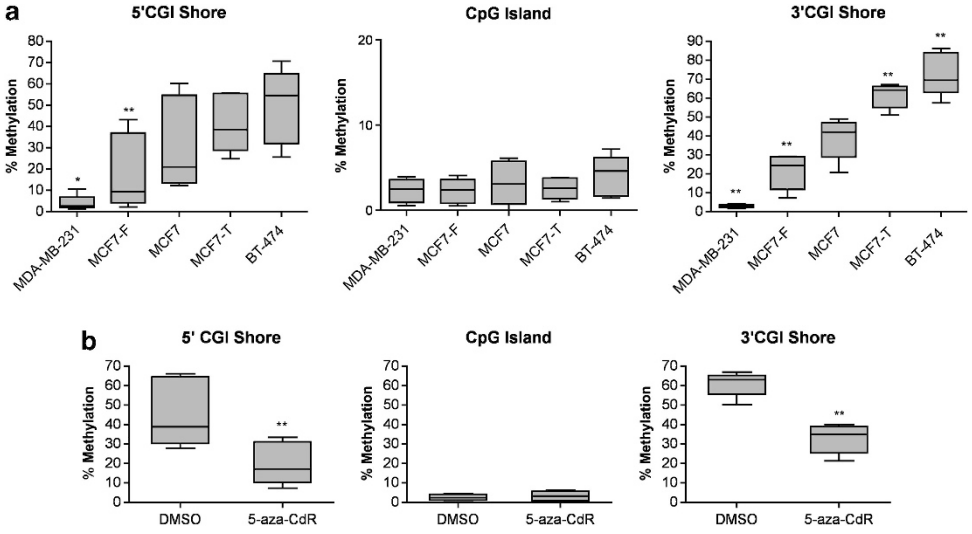

Figure 3. Differential Cav1 CGI shore methylation in antiestrogen-resistant breast cancer cell lines. (**a**) The box-and-whisker plot displays pyrosequencing results of five cell lines. The methylation level is indicated as percentage: 0, no methylation; 100, 100% methylation of the CpG sites. The statistical analysis was performed for MCF7 vs all other cell lines. $^{**}P<0.01$. For methylation of 3′-CGI shore, all the cell lines were different from each other ($P<0.01$), except for MCF7-T vs BT474. (**b**) The box-and-whisker plot displays pyrosequencing results of MCF7-T cells after treating with 5 μM 5-aza-CdR for 6 days. $^{**}P<0.01$.

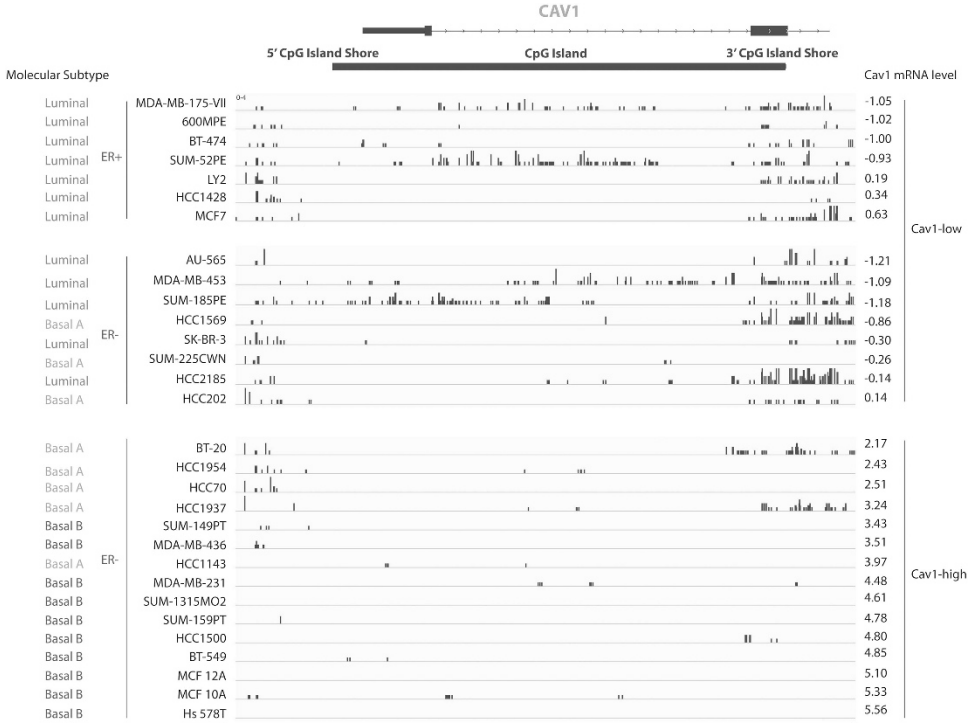

Figure 4. IGV (Integrative Genomics Viewer) view of sequenced DNA methylation tracks of 30 breast cancer cell lines. Top, Cav1 transcript, Cav1 CGI and CGI shores; Right, Cav1 expression for each cell line, according to previously published data;[21] Left, subtype and ERα expression of each cell line. Numbers on right are Log2 expression ratio normalized to the mean of Cav1 expression in all cell lines.

hypothesize that Cav1 CGI shore hypomethylation likely contributes to enhanced aggressiveness of these cells.

Cav1 methylation and expression in breast tumors from breast cancer patients

To investigate whether Cav1 CGI shore methylation also occurs in human breast tumors, we performed genome-wide profiling of DNA methylation on 77 breast tumors (50 ERα-positive and 27 ERα-negative, Supplementary Table S2) and 10 normal breast tissues. In normal breast tissues, hypomethylation of both Cav1 CGI and CGI shores was observed (Figure 7), consistent with previously reported high Cav1 expression in normal breast tissues.[16,17] The majority of ERα-positive tumors displayed hypermethylation of the Cav1 3′CGI shore, varied methylation of 5′-CGI shore, and sporadic hypermethylation of Cav1 CGI

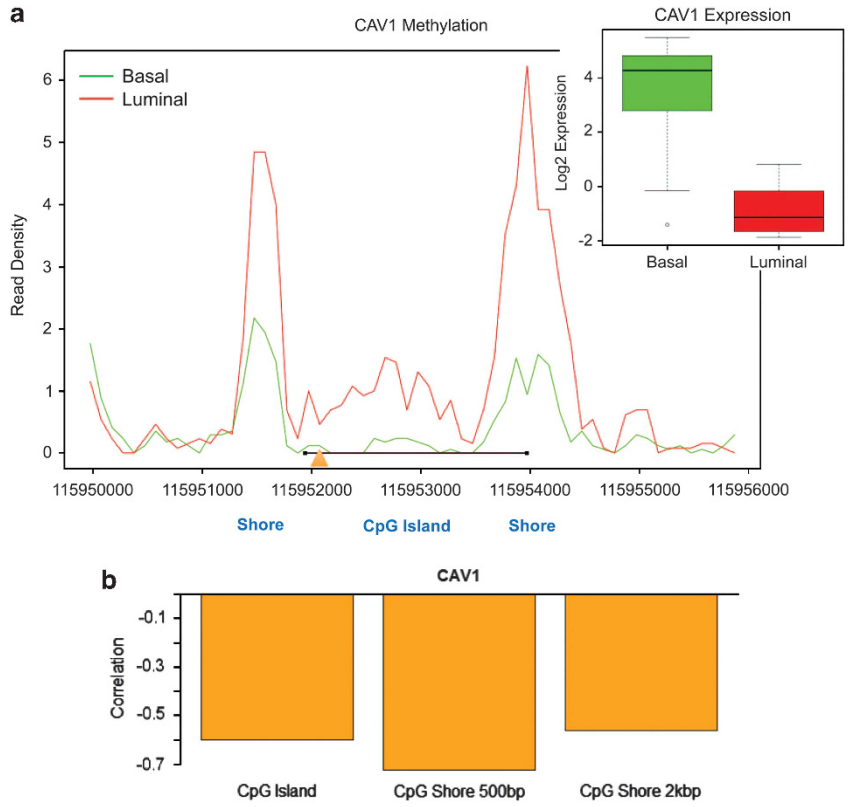

Figure 5. Negative correlation of Cav1 CGI shore methylation and Cav1 expression. (**a**) Integrated methylation results of 30 breast cancer cell lines. The *x*-axis represents nucleotide position according to human reference genome (hg18). The *y*-axis represents read density of CpG methylation level: the green line shows the methylation results of 18 basal-like breast cancer cell lines and the red line indicates the methylation results of 12 luminal breast cancer cell lines. The Cav1 transcription start site is indicated by the orange triangle. The location of the Cav1 CGI is indicated by the black line. The box-and-whisker plot displays Cav1 expression level in all basal-like cell lines (green bar) and luminal cell lines (red bar). $^{**}P<0.01$. (**b**) Bar plot of the Pearson correlation coefficient (*r*) showing the strength of the negative correlation between Cav1 expression and methylation on CGI, CGI shore within 500 bp, and CGI shore within 2 kb. All three correlations were significantly negative ($P<0.05$), but only methylation of CGI shore within 500 bp showed a strong negative association with Cav1 expression ($r<-0.7$).

(Figure 6). In the ERα-negative tumors, Cav1 promoter CGI hypomethylation was apparent, but shore methylation varied among the individual samples (Figure 6). Statistical analysis confirmed hypomethylation of Cav1 CGI in both ERα-positive and -negative breast tumors, although ERα-positive tumors had significantly higher methylation levels (median 0.1 vs 0, $P=0.009$, Figure 7). Cav1 5′-CGI shore methylation levels were variable, with no difference between ERα-positive and -negative tumors ($P=0.64$, Figure 7). However, Cav1 3′-CGI shore was heavily methylated and the methylation levels were significantly higher in ERα-positive tumors ($P=0.045$, Figure 7). Owing to lack of gene expression data, we were not able to associate Cav1 CGI shore methylation with Cav1 expression in this cohort of patients. However, using the Kaplan–Meier Plotter tool,[41] we found that Cav1 expression was associated with overall survival rates for breast cancer patients with ERα-negative tumors (total patient number = 63, *P*-value = 0.028) (Figure 8a). This association was also observed in ERα-negative, grade 3 patients (total patient number = 47, *P*-value = 0.037) (Figure 8b).

DISCUSSION

Cav1 expression has been associated with basal-like breast cancer.[22] In the current study, we demonstrate, for the first time, alteration of Cav1 expression when a breast cancer cell line changes from luminal subtype (MCF7) to basal-like (MCF7-F), using a previously established breast cancer model.[33] We further demonstrate an oncogenic role for Cav1 in basal-like cell lines, by enhancing cell proliferation, anchorage-independent growth, migration and invasion (Figure 1). In agreement with a new understanding of the role of CGI shore methylation in cancer,[30] previously considered a mere extension of CGI methylation, we report, for the first time, a strong association between CGI shore methylation and Cav1 expression in breast cancer and confirm this unique methylation pattern in a panel of 30 breast cancer cell lines (Figures 2–5). We further show that Cav1 CGI shores are hypomethylated in the basal subtype of breast cancer cell lines (Figure 5), supporting its association with tumor progression. In human breast tumors, Cav1 3′-CGI shore is more often hypermethylated in ERα-positive tumors than in ERα-negative tumors (Figures 6 and 7). The correlation of Cav1 expression and clinical outcome (Figure 8) suggests that Cav1 may represent a novel prognostic factor for ERα-negative, basal-like breast cancer.

The function of Cav1 in cancer is cell context dependent.[10] In ERα-positive breast cancer cells, Cav1 has a tumor-suppressive role. Estradiol treatment reduces Cav1 expression to promote cell proliferation,[18,42] and MCF7 cells stably overexpressing Cav1 exhibit reduced cell growth, colony formation and invasiveness.[43] However, in ERα-negative basal-like breast cancer cells, Cav1 switches to an oncogenic role. It can elevate insulin growth factor-I (IGF-I) receptor transcription[44] to promote cell proliferation or become phosphorylated at tyrosine 14 to enhance anchorage-independent growth and promotes tumor cell migration.[45] Here, we illustrated that the switch of the role of Cav1 is accompanied with Cav1 upregulation, as well as Cav1 CGI shore demethylation.

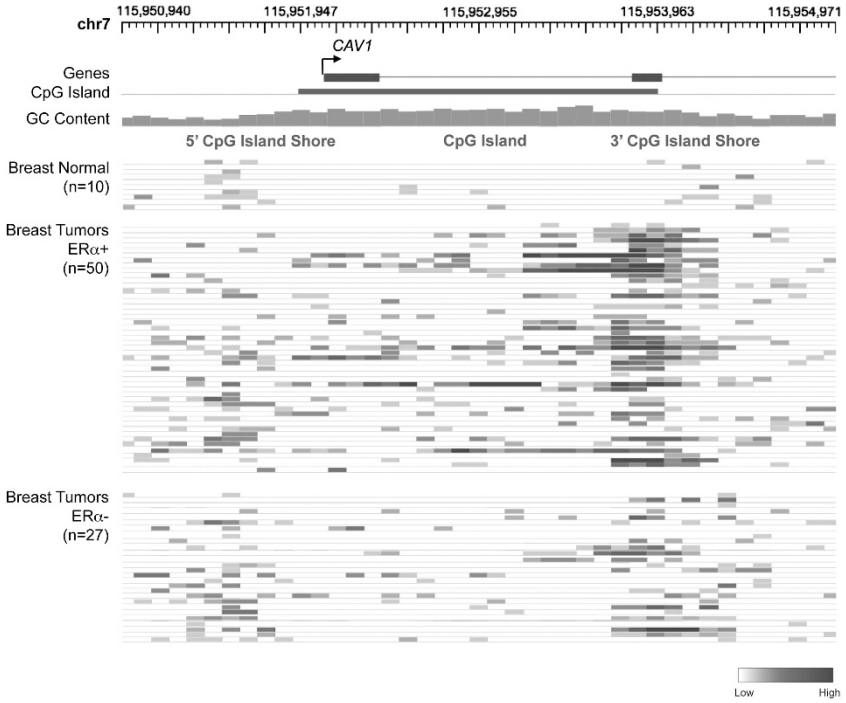

Figure 6. The Cancer Methylome System (CMS) view of sequenced DNA methylation tracks of 77 breast tumors and 10 normal breast tissues. The gray squares represent methylation level of CpG sites, as indicated by the scale (dark, high; light, low).

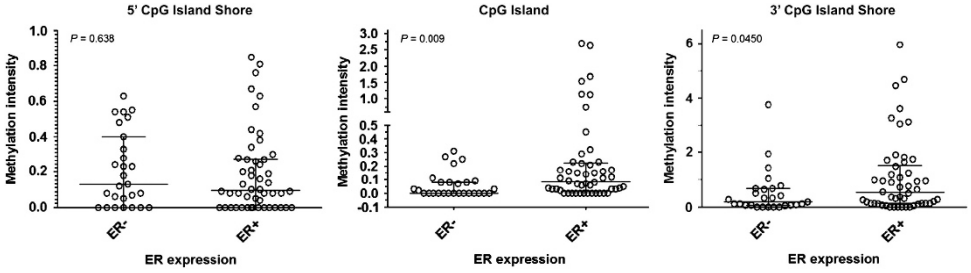

Figure 7. Dot plots of Cav1 promoter methylation in human breast tumors. As Cav1 CGI shore methylation extends into part of the CpG island (CGI), the 5′-CGI shore analyzed here covers 500 bp upstream of CGI and 250 bp in the 5′ CGI. The 3′-CGI shore covers 500 bp downstream of CGI and 250 bp in the 3′ CGI. The CGI covers the center 1.5 kb CGI region. The black lines indicate medium (middle) and interquartile range (two ends). Two-sided Mann–Whitney test was used to analyze statistic significance and *P*-values are as indicated.

Our conclusion that Cav1 expression is not strongly regulated by promoter CGI methylation is further confirmed by a recently reported breast cancer methylome study,[46] which used the Infinium platform covering CpG sites only in the Cav1 promoter CGI. As shown in Supplementary Table S3 five of the six CpG sites were hypomethylated and no association of methylation with Cav1 expression or clinical outcome was observed. Our observation of Cav1 CGI shore methylation is also consistent with several previous studies. Engelman *et al.*[47] reported Cav1 CGI methylation in breast cancer cell lines. However, the interrogated region in that study (-359 to -330 bp) was actually upstream of the currently defined Cav1 CGI. Methylation of seven CpG sites, located from -404 to -149 bp upstream of the CGI, within the 5′-CGI shore of Cav1 we studied, were sufficient to abolish Cav1 expression.[35,36,48] Cav1 3′-CGI shore methylation has not been reported previously, perhaps because this region surrounds the second exon of Cav1, while previous studies examined whether promoter/first exon methylation correlated with Cav1 transcriptional silencing. However, because of alternative splicing, Cav1 has four transcript variants encoding α and β isoforms, transcribed from the 5′UTR (variant 1, isoform α) or upstream of the second exon (variant 2/3/4, isoform β). We are currently investigating whether the 3′-CGI shore methylation may also regulate isoform expression.

To examine whether the Cav1 CGI chromatin environment (and shore regions) associates with Cav1 expression, we performed ChIP-seq analysis for histone tail modifications in MCF7 and MCF7-T (both Cav1-low cell lines; Figure 1). In MCF7, high level of H3K4me2 enrichment was observed at the Cav1 CGI region, with minimal enrichment of this active mark in the CGI shore (Supplementary Figure S13). Enrichment of H3K9me2 was only observed at Cav1 3′-CGI shore, while H3K27me3 occupied both Cav1 5′- and 3′-CGI shores. Similar enrichment of H3K4me2 at the Cav1 CGI region in MCF7-T cells was seen; however, H3K9me2 and H3K27me3 repressive marks accrued at the center of the CGI region and 3′-CGI shore (Supplementary Figure S13). Combined with the above results, H3K4me2 enrichment in the Cav1 CGI does not appear sufficient to activate Cav1 transcription in MCF7 and MCF7-T cells, thus suggesting a need for other factors. On the other hand, H3K4me2 occupancy on Cav1 CGI may contribute to the CGI hypomethylation, as H3K4 methylation inhibits *de novo* DNA methylation.[49]

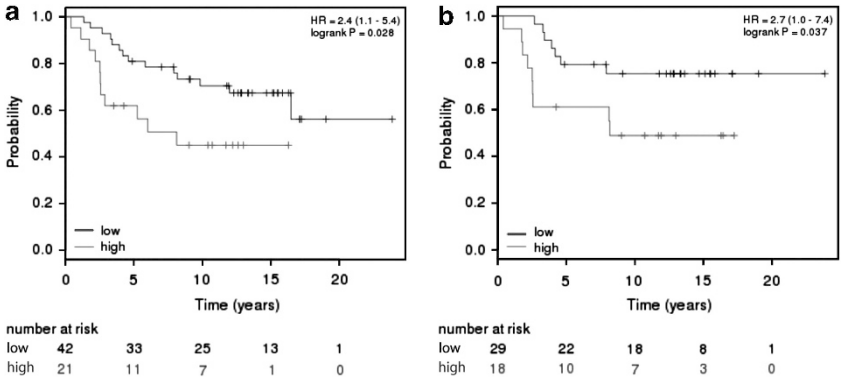

Figure 8. Relationship of Cav1 expression and overall survival of breast cancer patients. (**a**) Survival analysis indicating significantly worse overall survival of patients with ERα-negative tumors expressing higher level of Cav1 (total patient number = 63, *P*-value = 0.028). (**b**) Survival analysis indicating significantly worse overall survival of ERα-negative, grade 3 patients (total patient number = 47, *P*-value = 0.037).

In breast cancer, Cav1 expression is strongly negatively correlated with ERα expression,[50] and ERα has been reported to silence Cav1.[48] It has been reported that treatment with estradiol[18,42] decreases Cav1 expression. We also observed that tamoxifen (Figure 1c), which stabilizes ERα protein level,[51] reduced Cav1 expression in MCF7 cells. ERα protein levels are increased in tamoxifen-resistant breast cancer cell lines,[33,52] and Cav1 expression is further repressed in MCF7-T compared with MCF7 (Figure 1a), along with an increase in CGI shore methylation (Figure 3a). Taken together, these observations indicate that ERα may be the primary factor contributing to Cav1 CGI shore methylation and repressed Cav1 expression in ERα-positive breast cancer. However, CGI shore methylation appears to permanently silence Cav1, as short-term treatment of MCF7 cells with fulvestrant, which induces rapid ERα degradation,[51] has no effect on Cav1 levels[48] (Figure 1c). During the development of stable fulvestrant resistance and the ERα-negative, basal-like phenotype, Cav1 CGI shore hypomethylation appears to be induced by an unknown mechanism(s) that may warrant further investigation.

No association between Cav1 expression and overall survival was observed when the entire breast cancer cohort was used in the analysis (Supplementary Figure S14), consistent with a previous report[50] and the fact that over 70% of breast cancer in the cohort are ERα positive and display low Cav1 expression. However, our subgroup analysis revealed that elevated Cav1 levels in more aggressive ERα-negative patients associated with shorter overall survival (Figure 7a). Further subgrouping of the cohort to grade 3 breast cancer resulted in a similar negative association (Figure 7b). These results imply that Cav1 expression may serve as a prognostic factor for ERα-negative and high-grade breast cancer patients. However, it should be noted that the number of patients with ERα-negative breast cancer and Cav1 expression was limited. In addition, cohort differences may affect the results, as a recent study identified Cav1 as an independent prognostic factor for invasive breast carcinoma.[53]

In this the first report of an oncogenic role for Cav1 in basal-like breast cancer, and first comprehensive analysis of Cav1 methylation, we reveal a negative relationship between Cav1 CGI shore methylation and Cav1 expression in breast cancer. Our findings support a previously described role for CGI shore methylation in cancer,[30] demonstrating the importance of including CGI shores in future DNA methylome analyses. We specifically demonstrate an association between Cav1 CGI shore methylation and breast tumor progression. The correlation of Cav1 level and clinical outcome further suggests that Cav1 expression and Cav1 CGI shore methylation may represent novel prognostic factors for ERα-negative, basal-like breast cancer.

MATERIALS AND METHODS

Cell lines and reagents

Breast cancer cell lines were obtained from American Type Culture Collection (Manassas, VA, USA) and cultured according to the protocols provided by the company. MCF7, MCF7-T, and MCF7-F cells were cultured as previously described.[33] 5-Aza-2′-deoxycytidine (5-aza-CdR) was purchsed from Sigma-Aldrich Co. LLC (St Louis, MO, USA). Small interfering RNAs that target Cav1 were from Santa Cruz Biotechnology Inc. (Santa Cruz, CA, USA). pCMV6-XL5 (vector) and pCav1 (plasmid that overexpresses Cav1) were purchased from OriGene Technologies Inc. (Rockville, MD, USA). Anti-Cav1 (clone 2297) antibody was from BD Biosciences (San Diego, CA, USA).

Transfection, cell viability assay and clonogenicity assays

Plasmids were transfected with Eugene HD Transfection Reagent (Roche Applied Science, Indianapolis, IN, USA), and Lipofectamine 2000 (Invitrogen, Carlsbad, CA, USA) was used for small interfering RNA transfections. Cell viability was determined by the 3-(4,5-dimethylthiazol-2-yl)-2,5-diphenyltetrazolium bromide (MTT, Sigma-Aldrich) assay, as described previously.[33] To examine clonogenic activity, cells were seeded (300 er well) in six-well plates, cultured for 10–14 days, and then stained with 0.5% methylene blue in 50% methanol. Colonies containing $\geqslant$50 cells were scored.

Migration/invasion assays

Migration/invasion assays were performed according to previous description.[54] Transwell chambers (24-well; BD BioCoat Control Inserts from BD Biosciences) with 8.0-μm pore size polycarbonate membrane were used for migration assay, and BD BioCoat Matrigel Invasion Chamber (BD Biosciences) was used for invasion assays. Migrated and invaded cells were stained and observed under the optical microscope at a magnification of $\times$100. Cells were counted in 5 fields of triplicate membranes. See Supplementary Materials for details.

DNA extraction and bisulphite conversion

Genomic DNA was isolated using QIAmp DNA Blood Mini Kit (Qiagen, Valencia, CA, USA), as described previously.[55] Sodium bisulfite conversion and cleanup were performed using EZ DNA Methylation kit (Zymo Research, Orange, CA, USA), according to the manufacturer's instruction.

Methylation specific PCR and bisulfite genomic DNA sequencing

DNA methylation on the Cav1 CGI and 5′-CGI shore was determined using methylation-specific PCR according to previous description.[35,38] Methylated and unmethylated control DNAs were purchased from Qiagen. Bisulfite genomic DNA sequencing was used to determine methylation of Cav1 CGI, as described previously.[35] See Supplementary Materials for details.

DNA methylation analysis by pyrosequencing

The Pyro Mark Assay Design program (Qiagen) was used to design primers for amplification of specific regions of Cav1 CGI and CGI shores from bisulfite-converted genomic DNA (Supplementary Table S1). The methylation level of individual CpG sites in each amplicon was detected using Pyrosequencing system[56] and analyzed by the Pyro Q-CpG software. Box-and-whisker plots, generated in GraphPad Prism version 4.0 (GraphPad Software, San Diego, CA, USA) using default settings, were used to display the methylation results. The boxes show the interquartile range (IQR) around the median; the whiskers extend from the minimum value to the maximum value.

Methyl-CpG binding domain-based capture coupled with massively parallel sequencing and identification of differentially methylated regions

Methyl-CpG binding domain protein sequencing was performed for 30 breast cancer cell lines, 77 breast tumors (Supplementary Table S2) and 10 normal breast tissues as previously described.[32,57,58] The genome-wide methylation data were processed using mCpG-SNP-EXPRESS (Chae *et al.* unpublished). MACS[59] was used to identify differentially methylated regions in breast cancer cell lines. The bi-asymmetric-Lapilace model[58] was used to identify differentially methylated regions in breast tumors. See Supplementary Materials for details. The methylome data set is available at ''The Cancer Methylome System'' website: http://cbbiweb.uthscsa.edu/KMethylomes/.

Correlation analysis

A Pearson correlation one-tailed *t*-test was performed to measure the association between the gene expression and methylation. A P-value < 0.05 was considered significant. Correlation coefficients (*r values*) from -1.0 to -0.7 represented a strong negative association, with r value from -0.7 to -0.3 considered weak negative associations and r values from -0.3 to $+0.3$ indicating little or no association.

RNA-seq

For whole transcriptome analysis, RNA-seq libraries were generated utilizing a modified version of the Illumina directional mRNA-seq library protocol with duplex specific nuclease (DSN; Evrogen, Moscow, Russia) normalization (Nephew and co-workers, manuscript in preparation). Next generation sequencing was performed with the Illumina GAII analyzer. Sequence reads (51 bp) were mapped to the human genome (NCBI36/hg18) using the Solexa Analysis Pipeline with BFAST alignments and a TopHat-like strategy to determine splicing junctions followed by expression level (RPKM) analyses with Cufflinks.[60] See Supplementary Materials for details.

Kaplan–Meier survival analysis

The association of Cav1 expression and overall survival rate in breast cancer patients was analyzed using an online survival analysis tool, Kaplan–Meier Plotter (http://kmplot.com/backup/breast). It assesses the effect of gene expression on breast cancer prognosis using microarray data from 1809 patients.[41] The patient data are from GEO, with available raw data and clinical survival information),

Statistical analysis

For MTT cell viability, clonogenicity, quantitative reverse transcription–PCR, and migration/invasion assays, statistical significance was analyzed by unpaired Student's *t*-test. For the methylation results (box-and-whisker plots), paired Student's *t*-test was performed. P-values < 0.05 were considered statistically significant. For Cav1 promoter methylation in breast tumors, statistical significance was analyzed by two-sided Mann–Whitney test.

CONFLICT OF INTEREST

The authors declare no conflict of interest.

ACKNOWLEDGEMENTS

The authors wish to thank Dr F Fang for pyrosequencing analysis, Dr C Balch for manuscript preparation, and the IUB light Microscopy Imaging Center for microscopy resources. This work was supported by NIH grants CA085289 and CA113001, pilot project funding from the Integrated Cancer Biology Program and the Walther Cancer Foundation (Indianapolis, IN, USA). We acknowledge the use of the ICBP45 Kit in this study.

REFERENCES

1 Razani B, Woodman SE, Lisanti MP. Caveolae: from cell biology to animal physiology. *Pharmacol Rev* 2002; **54**: 431–467.
2 Liu P, Rudick M, Anderson RG. Multiple functions of caveolin-1. *J Biol Chem* 2002; **277**: 41295–41298.
3 Li S, Couet J, Lisanti MP. Src tyrosine kinases, Galpha subunits, and H-Ras share a common membrane-anchored scaffolding protein, caveolin. Caveolin binding negatively regulates the auto-activation of Src tyrosine kinases. *J Biol Chem* 1996; **271**: 29182–29190.
4 Couet J, Sargiacomo M, Lisanti MP. Interaction of a receptor tyrosine kinase, EGF-R, with caveolins. Caveolin binding negatively regulates tyrosine and serine/threonine kinase activities. *J Biol Chem* 1997; **272**: 30429–30438.
5 Ostrom RS, Insel PA. The evolving role of lipid rafts and caveolae in G protein-coupled receptor signaling: implications for molecular pharmacology. *Br J Pharmacol* 2004; **143**: 235–245.
6 Engelman JA, Wykoff CC, Yasuhara S, Song KS, Okamoto T, Lisanti MP. Recombinant expression of caveolin-1 in oncogenically transformed cells abrogates anchorage-independent growth. *J Biol Chem* 1997; **272**: 16374–16381.
7 Patel HH, Murray F, Insel PA. Caveolae as organizers of pharmacologically relevant signal transduction molecules. *Annu Rev Pharmacol Toxicol* 2008; **48**: 359–391.
8 Engelman JA, Zhang XL, Galbiati F, Lisanti MP. Chromosomal localization, genomic organization, and developmental expression of the murine caveolin gene family (Cav-1, -2, and -3). Cav-1 and Cav-2 genes map to a known tumor suppressor locus (6-A2/7q31). *FEBS Lett* 1998; **429**: 330–336.
9 Shatz M, Liscovitch M. Caveolin-1: a tumor-promoting role in human cancer. *Int J Radiat Biol* 2008; **84**: 177–189.
10 Goetz JG, Lajoie P, Wiseman SM, Nabi IR. Caveolin-1 in tumor progression: the good, the bad and the ugly. *Cancer Metastasis Rev* 2008; **27**: 715–735.
11 Nestl A, Von Stein OD, Zatloukal K, Thies WG, Herrlich P, Hofmann M *et al.* Gene expression patterns associated with the metastatic phenotype in rodent and human tumors. *Cancer Res* 2001; **61**: 1569–1577.
12 Tse EY, Ko FC, Tung EK, Chan LK, Lee TK, Ngan ES *et al.* Caveolin-1 overexpression is associated with hepatocellular carcinoma tumorigenesis and metastasis. *J Pathol* 2011; **226**: 645–653.
13 Arpaia E, Blaser H, Quintela-Fandino M, Duncan G, Leong HS, Ablack A *et al.* The interaction between caveolin-1 and Rho-GTPases promotes metastasis by controlling the expression of alpha5-integrin and the activation of Src, Ras and Erk. *Oncogene* 2011; **31**: 884–896.
14 Ravid D, Maor S, Werner H, Liscovitch M. Caveolin-1 inhibits cell detachment-induced p53 activation and anoikis by upregulation of insulin-like growth factor-I receptors and signaling. *Oncogene* 2005; **24**: 1338–1347.
15 Belanger MM, Roussel E, Couet J. Up-regulation of caveolin expression by cytotoxic agents in drug-sensitive cancer cells. *Anticancer Drugs* 2003; **14**: 281–287.
16 Park SS, Kim JE, Kim YA, Kim YC, Kim SW. Caveolin-1 is down-regulated and inversely correlated with HER2 and EGFR expression status in invasive ductal carcinoma of the breast. *Histopathology* 2005; **47**: 625–630.
17 Sagara Y, Mimori K, Yoshinaga K, Tanaka F, Nishida K, Ohno S *et al.* Clinical significance of Caveolin-1, Caveolin-2 and HER2/neu mRNA expression in human breast cancer. *Br J Cancer* 2004; **91**: 959–965.
18 Thomas NB, Hutcheson IR, Campbell L, Gee J, Taylor KM, Nicholson RI *et al.* Growth of hormone-dependent MCF-7 breast cancer cells is promoted by constitutive caveolin-1 whose expression is lost in an EGF-R-mediated manner during development of tamoxifen resistance. *Breast Cancer Res Treat* 2010; **119**: 575–591.
19 Savage K, Lambros MB, Robertson D, Jones RL, Jones C, Mackay A *et al.* Caveolin 1 is overexpressed and amplified in a subset of basal-like and metaplastic breast carcinomas: a morphologic, ultrastructural, immunohistochemical, and in situ hybridization analysis. *Clin Cancer Res* 2007; **13**: 90–101.
20 Van den Eynden GG, Van Laere SJ, Van der Auwera I, Merajver SD, Van Marck EA, van Dam P *et al.* Overexpression of caveolin-1 and -2 in cell lines and in human samples of inflammatory breast cancer. *Breast Cancer Res Treat* 2006; **95**: 219–228.
21 Neve RM, Chin K, Fridlyand J, Yeh J, Baehner FL, Fevr T *et al.* A collection of breast cancer cell lines for the study of functionally distinct cancer subtypes. *Cancer Cell* 2006; **10**: 515–527.
22 Pinilla SM, Honrado E, Hardisson D, Benitez J, Palacios J. Caveolin-1 expression is associated with a basal-like phenotype in sporadic and hereditary breast cancer. *Breast Cancer Res Treat* 2006; **99**: 85–90.
23 Kao J, Salari K, Bocanegra M, Choi YL, Girard L, Gandhi J *et al.* Molecular profiling of breast cancer cell lines defines relevant tumor models and provides a resource for cancer gene discovery. *PLoS One* 2009; **4**: e6146.
24 Jones PA, Baylin SB. The epigenomics of cancer. *Cell* 2007; **128**: 683–692.

25 Jones PA, Liang G. Rethinking how DNA methylation patterns are maintained. *Nat Rev Genet* 2009; **10**: 805–811.
26 Herman JG, Baylin SB. Gene silencing in cancer in association with promoter hypermethylation. *N Engl J Med* 2003; **349**: 2042–2054.
27 Deaton AM, Bird A. CpG islands and the regulation of transcription. *Genes Dev* 2011; **25**: 1010–1022.
28 Rollins RA, Haghighi F, Edwards JR, Das R, Zhang MQ, Ju J *et al.* Large-scale structure of genomic methylation patterns. *Genome Res* 2006; **16**: 157–163.
29 Han H, Cortez CC, Yang X, Nichols PW, Jones PA, Liang G. DNA methylation directly silences genes with non-CpG island promoters and establishes a nucleosome occupied promoter. *Hum Mol Genet* 2011; **20**: 4299–4310.
30 Irizarry RA, Ladd-Acosta C, Wen B, Wu Z, Montano C, Onyango P *et al.* The human colon cancer methylome shows similar hypo- and hypermethylation at conserved tissue-specific CpG island shores. *Nat Genet* 2009; **41**: 178–186.
31 Doi A, Park IH, Wen B, Murakami P, Aryee MJ, Irizarry R *et al.* Differential methylation of tissue- and cancer-specific CpG island shores distinguishes human induced pluripotent stem cells, embryonic stem cells and fibroblasts. *Nat Genet* 2009; **41**: 1350–1353.
32 Serre D, Lee BH, Ting AH. MBD-isolated Genome Sequencing provides a high-throughput and comprehensive survey of DNA methylation in the human genome. *Nucleic Acids Res* 2010; **38**: 391–399.
33 Fan M, Yan PS, Hartman-Frey C, Chen L, Paik H, Oyer SL *et al.* Diverse gene expression and DNA methylation profiles correlate with differential adaptation of breast cancer cells to the antiestrogens tamoxifen and fulvestrant. *Cancer Res* 2006; **66**: 11954–11966.
34 Wiechen K, Diatchenko L, Agoulnik A, Scharff KM, Schober H, Arlt K *et al.* Caveolin-1 is down-regulated in human ovarian carcinoma and acts as a candidate tumor suppressor gene. *Am J Pathol* 2001; **159**: 1635–1643.
35 Sunaga N, Miyajima K, Suzuki M, Sato M, White MA, Ramirez RD *et al.* Different roles for caveolin-1 in the development of non-small cell lung cancer versus small cell lung cancer. *Cancer Res* 2004; **64**: 4277–4285.
36 Bachmann N, Haeusler J, Luedeke M, Kuefer R, Perner S, Assum G *et al.* Expression changes of CAV1 and EZH2, located on 7q31 approximately q36, are rarely related to genomic alterations in primary prostate carcinoma. *Cancer Genet Cytogenet* 2008; **182**: 103–110.
37 Chan TF, Su TH, Yeh KT, Chang JY, Lin TH, Chen JC *et al.* Mutational, epigenetic and expressional analyses of Caveolin-1 gene in cervical cancers. *Int J Oncol* 2003; **23**: 599–604.
38 Lin SY, Yeh KT, Chen WT, Chen HC, Chen ST, Chang JG. Promoter CpG methylation of caveolin-1 in sporadic colorectal cancer. *Anticancer Res* 2004; **24**: 1645–1650.
39 Hurlstone AF, Reid G, Reeves JR, Fraser J, Strathdee G, Rahilly M *et al.* Analysis of the CAVEOLIN-1 gene at human chromosome 7q31.1 in primary tumours and tumour-derived cell lines. *Oncogene* 1999; **18**: 1881–1890.
40 Patani N, Lambros MB, Natrajan R, Dedes KJ, Geyer FC, Ward E *et al.* Non-existence of caveolin-1 gene mutations in human breast cancer. *Breast Cancer Res Treat* 2012; **131**: 307–310.
41 Gyorffy B, Lanczky A, Eklund AC, Denkert C, Budczies J, Li Q *et al.* An online survival analysis tool to rapidly assess the effect of 22,277 genes on breast cancer prognosis using microarray data of 1809 patients. *Breast Cancer Res Treat* 2010; **123**: 725–731.
42 Razandi M, Oh P, Pedram A, Schnitzer J, Levin ER. ERs associate with and regulate the production of caveolin: implications for signaling and cellular actions. *Mol Endocrinol* 2002; **16**: 100–115.
43 Fiucci G, Ravid D, Reich R, Liscovitch M. Caveolin-1 inhibits anchorage-independent growth, anoikis and invasiveness in MCF-7 human breast cancer cells. *Oncogene* 2002; **21**: 2365–2375.
44 Glait C, Tencer L, Ravid D, Sarfstein R, Liscovitch M, Werner H. Caveolin-1 up-regulates IGF-I receptor gene transcription in breast cancer cells via Sp1- and p53-dependent pathways. *Exp Cell Res* 2006; **312**: 3899–3908.
45 Williams TM, Lisanti MP. Caveolin-1 in oncogenic transformation, cancer, and metastasis. *Am J Physiol Cell Physiol* 2005; **288**: C494–C506.
46 Fackler MJ, Umbricht CB, Williams D, Argani P, Cruz LA, Merino VF *et al.* Genome-wide methylation analysis identifies genes specific to breast cancer hormone receptor status and risk of recurrence. *Cancer Res* 2011; **71**: 6195–6207.
47 Engelman JA, Zhang XL, Lisanti MP. Sequence and detailed organization of the human caveolin-1 and -2 genes located near the D7S522 locus (7q31.1). Methylation of a CpG island in the 5′ promoter region of the caveolin-1 gene in human breast cancer cell lines. *FEBS Lett* 1999; **448**: 221–230.
48 Zschocke J, Manthey D, Bayatti N, van der Burg B, Goodenough S, Behl C. Estrogen receptor alpha-mediated silencing of caveolin gene expression in neuronal cells. *J Biol Chem* 2002; **277**: 38772–38780.
49 Ooi SK, Qiu C, Bernstein E, Li K, Jia D, Yang Z *et al.* DNMT3L connects unmethylated lysine 4 of histone H3 to *de novo* methylation of DNA. *Nature* 2007; **448**: 714–717.
50 Elsheikh SE, Green AR, Rakha EA, Samaka RM, Ammar AA, Powe D *et al.* Caveolin 1 and Caveolin 2 are associated with breast cancer basal-like and triple-negative immunophenotype. *Br J Cancer* 2008; **99**: 327–334.
51 Wijayaratne AL, McDonnell DP. The human estrogen receptor-alpha is a ubiquitinated protein whose stability is affected differentially by agonists, antagonists, and selective estrogen receptor modulators. *J Biol Chem* 2001; **276**: 35684–35692.
52 Pink JJ, Jiang SY, Fritsch M, Jordan VC. An estrogen-independent MCF-7 breast cancer cell line which contains a novel 80-kilodalton estrogen receptor-related protein. *Cancer Res* 1995; **55**: 2583–2590.
53 Joshi B, Strugnell SS, Goetz JG, Kojic LD, Cox ME, Griffith OL *et al.* Phosphorylated caveolin-1 regulates Rho/ROCK-dependent focal adhesion dynamics and tumor cell migration and invasion. *Cancer Res* 2008; **68**: 8210–8220.
54 Rosman DS, Phukan S, Huang CC, Pasche B. TGFBR1*6A enhances the migration and invasion of MCF-7 breast cancer cells through RhoA activation. *Cancer Res* 2008; **68**: 1319–1328.
55 Fang F, Balch C, Schilder J, Breen T, Zhang S, Shen C *et al.* A phase 1 and pharmacodynamic study of decitabine in combination with carboplatin in patients with recurrent, platinum-resistant, epithelial ovarian cancer. *Cancer* 2010; **116**: 4043–4053.
56 Tost J, Gut IG. DNA methylation analysis by pyrosequencing. *Nat Protoc* 2007; **2**: 2265–2275.
57 Zuo T, Liu TM, Lan X, Weng YI, Shen R, Gu F *et al.* Epigenetic silencing mediated through activated PI3K/AKT signaling in breast cancer. *Cancer Res* 2011; **71**: 1752–1762.
58 Lan X, Adams C, Landers M, Dudas M, Krissinger D, Marnellos G *et al.* High resolution detection and analysis of CpG dinucleotides methylation using MBD-Seq technology. *PLoS One* 2011; **6**: e22226.
59 Zhang Y, Liu T, Meyer CA, Eeckhoute J, Johnson DS, Bernstein BE *et al.* Model-based analysis of ChIP-Seq (MACS). *Genome Biol* 2008; **9**: R137.
60 Patani N, Martin LA, Reis-Filho JS, Dowsett M. The role of caveolin-1 in human breast cancer. *Breast Cancer Res Treat* 2012; **131**: 1–15.

Supplementary Information accompanies the paper on the Oncogene website (http://www.nature.com/onc)